Impact of the QBO on prediction and predictability of the MJO convection

Shuguang Wang[1]
Michael K. Tippett[1]
Adam H. Sobel[1,2]
Zane Martin[1]
Frederic Vitart[3]

1 Department of Applied Physics and Applied Mathematics, Columbia University, New York, NY

2 Lamont-Doherty Earth Observatory of Columbia University, Palisades, NY

3 European Centre for Medium-Range Weather Forecasts, Reading, UK

Submitted to

Journal of Geophysical Research - Atmosphere

2019

Key points:

1. MJO prediction skill higher by 5-10 days in QBO easterly than QBO westerly in the WMO/S2S models

2. Model forecasted stratosphere has little influence in MJO prediction

3. BSISO prediction skill higher in QBO westerly in 1999-2010 due to decadal variability of BSISO

Corresponding author: Shuguang Wang, Department of Applied Physics and Applied Mathematics, Columbia University, New York, NY 10025, sw2526@columbia.edu

Abstract

The impact of the QBO on the prediction of tropical intraseasonal convection, including the Madden Julian Oscillation (MJO) and Boreal Summer Intraseasonal Oscillation (BSISO), is assessed in the WMO Subseasonal to Seasonal (S2S) forecast database using the real-time OLR based MJO (ROMI) index. It is shown that the ROMI prediction skill for the boreal winter MJO, measured by the maximum time at which the anomaly correlation coefficient exceeds 0.6, is higher by 5 to 10 days in the QBO easterly phase than its westerly phase. This difference occurs even in models with low tops and poorly resolved stratospheres. MJO predictability as measured by signal to noise ratio also shows a similar difference between the two QBO phases, and results from a simple linear regression model show consistent behavior as well. Analysis of the OMI index derived from observations indicates that the MJO is more coherent and stronger in the QBO easterly phase than in the westerly phase. These results suggest that the skill dependence on MJO phase results from the initial state of the MJO, its persistence in the verifying observations, or most likely a combination of the two, but not on an actual stratospheric influence on the MJO within the model simulations.

In contrast to the robust QBO-MJO connection in boreal winter, the BSISO prediction skill by the S2S models in boreal summer is greater in QBO *westerly* phases than *easterly* phases during the 1999 to 2010 period. This is consistent with the observation that BSISO OLR anomalies are stronger in the QBO westerly phase in the same period. However, this relationship between the QBO and BSISO in boreal summer changes in recent decades: BSISO is weaker in QBO westerly than easterly during 1979-2000. Correspondingly, the QBO impact on MJO prediction in boreal summer also reverses in

25 that period as well in a statistical model, whereas this statistical model shows a consistent
26 QBO impact on MJO prediction in boreal winter over the past four decades.

1. Introduction

The Madden-Julian Oscillation (MJO; Madden and Julian 1971, 1972, Xie et al. 1963, Li et al. 2018) is the dominant mode of intraseasonal variability in the tropics. It influences weather directly over large regions of the tropics and subtropics, and its influence extends to the midlatitude and polar regions via Rossby wave trains excited by MJO convection. Understanding of the MJO's predictability is of great value.

One factor which has recently emerged as important to the MJO is the quasi-biennial oscillation (QBO; Baldwin et al. 2001) in the tropical stratosphere. A number of recent studies have found strong statistical relationships between the QBO phase and the amplitude of the MJO in northern winter. Yoo and Son (2016) and Son et al. (2017) showed that the MJO variance is higher in the QBO easterly phase (EQBO) than in the QBO westerly phase (WQBO) in boreal winter. Zhang and Zhang (2018) argued that the QBO has its strongest impact when the MJO convection is in the Maritime Continent.

These recent findings on the MJO-QBO connection have important consequences for MJO prediction. Marshall et al. (2017) showed that the QBO-MJO connection modulates MJO prediction skill in a subseasonal numerical weather prediction (NWP) model: MJO Real-Time Multivariate MJO (RMM, Wheeler and Hendon 2004) prediction skill is higher in the QBO easterly phase and lower in the QBO westerly phase. Marshall et al. (2017) also examined the QBO influence as a function of the initial amplitude of the MJO in the forecasts. They found that the difference in MJO prediction skill between QBO phases remains when forecasts with the same initial MJO amplitudes are compared, suggesting that the skill difference is not a simple consequence of higher amplitude MJO initial conditions in the easterly phase.

While studies to date are broadly consistent in finding a QBO influence on MJO prediction and predictability, understanding of this influence is limited. The QBO may influence both initial and boundary conditions, and their relative roles in influencing the MJO are not clear. For example, there is abundant evidence that air-sea turbulent fluxes at the lower boundary play important roles in the prediction of the MJO (DeMott et al. 2015). It is plausible that the QBO wind/temperature signature in the upper troposphere/lower stratosphere (UT/LS) region may reduce errors near the tropopause --- which we may think of as an "upper boundary" for the tropospheric MJO --- thereby improving prediction. On the other hand, given that there is a statistical relationship between QBO phase and MJO amplitude in observations, the QBO influence may be implicit in the tropospheric initial conditions, and influence the MJO prediction through that pathway. This influence could then be independent of the extent to which the QBO influences the MJO during the model run, or is even present in a given NWP model at all - especially considering that some NWP models have poorly-resolved stratospheres. It is desirable to understand whether this is the case, both to inform prediction and model development strategies (e.g., whether a well-resolved stratosphere is important to MJO prediction) and because it may help to understand the physical mechanism by which the QBO influences the MJO, which also remains unclear at present.

Another aspect of the MJO-QBO connection is the seasonal dependence of the QBO-MJO relationship. Yoo and Son (2016) found that the QBO-MJO relationship is significant in boreal winter but not in boreal summer. It is possible that this seasonal contrast is due to the distinctly different characteristics of the MJO in these two seasons. The intraseasonal oscillation mostly propagates eastward in northern winter, when its

convection anomalies are focused south of, but close to, the equator. In northern summer, when its convection anomalies are primarily found north of the equator, it propagates both northward and eastward, and reaches latitudes further from the equator than in northern winter. Because of these different characteristics, the MJO in summer is also referred to as the Boreal Summer Intraseasonal Oscillation (BSISO) in the literature. Densmore et al. (2018) further examined the QBO-MJO relationship in different seasons, and found – in addition to the documented signal in northern winter – that the QBO can also impact the MJO in other seasons in certain MJO phases, e.g., when the MJO convection is over the Maritime Continent in boreal spring and summer. It is of interest to see how this complex seasonality may influence the predictability of intraseasonal convective anomalies associated with the MJO and BSISO differently across the seasonal cycle.

The purpose of this study is to explore the QBO influence on the prediction and predictability of tropical intraseasonal convection anomalies using observations and the World Meteorological Organization's (WMO) S2S retrospective forecast dataset (Vitart et al. 2016). We use the real-time OLR based MJO index (OMI, or ROMI for the real-time variant; Kiladis et al. 2014) in order to focus on convection – as opposed to the circulation anomalies which are emphasized by some other indices, including the real time multivariate MJO index (Wheeler and Hendon 2004) – and we examine predictability across the seasonal cycle, including how it changes over the duration of the record.

The rest of this article is structured as follows: section 2 contains a brief description of the S2S models used here, the indices for diagnosing the MJO and QBO,

and a linear regression model for the MJO. Section 3 discusses the QBO impact on prediction and predictability of intreaseasonal convection anomalies. Section 4 summarizes this paper.

2. Method and the S2S data

2.1 The S2S prediction database

Reforecasts of the MJO were obtained from the WMO's Subseasonal-to-seasonal (S2S) Prediction Project database (Vitart et al. 2017). Most of the reforecasts are integrated for more than 30 days for subseasonal prediction. **Table 1** summarizes the forecast configurations of the 10 S2S models used in this study: the Australian Bureau of Meteorology (BoM), the China Meteorological Administration (CMA), the European Centre for Medium-Range Weather Forecasts (ECMWF), Environment and Climate Change Canada (ECCC), the Institute of Atmospheric Sciences and Climate of the National Research Council (CNR-ISAC), the Hydrometeorological Centre of Russia (HMCR), the Japan Meteorological Agency (JMA), Météo-France/Centre National de Recherche Meteorologiques (CNRM), the National Centers for Environmental Prediction (NCEP), and the Met Office (UKMO), including the horizontal and vertical resolution of their atmosphere components, model tops, reforecast types, forecast periods, reforecast frequencies, ensemble sizes, and ocean components (or lack thereof) . Among these models, 8 out of 10 are fully coupled Ocean and Atmosphere forecast systems, 2 are uncoupled (HMCR and ECCC), and 1 uses a slab ocean (ISAC). ECCC uses a persisted SST anomaly for the lower boundary condition.

These S2S models have very different representations of the stratosphere (Table 1): 3 out of 10 models (HMCR, BOM, ISAC) have relatively low model tops, with model top pressures greater than 10 hPa, while the rest have relatively high model tops.

2.2. The QBO index

We use the zonal mean zonal wind anomaly at 50 hPa (U50) averaged between 10°S and 10°N to diagnose the QBO. This NOAA QBO U50 index, available at http://www.cpc.ncep.noaa.gov/data/indices/qbo.u50.index, is highly asymmetric in the easterly and westerly phases, with more samples in westerly phases and fewer samples in easterly phase. To account for this asymmetry, we composite MJO indices using the 33.3 and 66.7 percentiles of the QBO U50 index: if U50 is less than -2.37 m/s, it is considered the QBO easterly phase (EQBO), and if U50 is greater than 5.13 m/s, it is counted as the QBO westerly phase (WQBO). For convenience, the MJO in the EQBO and WQBO will be referred to as MJO-EQBO and MJO-WQBO, respectively. This is justifiable because they differ significantly in amplitude, propagation speed, and period, as we shall see later.

2.3 The MJO index

We use the real-time variant of the OLR-based MJO index developed by Kiladis et al. (2014) to diagnose MJO convection in the S2S models. The OMI index complements the popular Real-Time Multivariate MJO (RMM, Wheeler and Hendon 2004) index for diagnosing the MJO activity. One advantage of OMI and ROMI is that, in addition to the MJO, these indices can track northward propagation of the intraseasonal convection in boreal summer, and hence are better suited for diagnosing the BSISO (Wang et al. 2018a). Wang et al. (2018b) described the technical details to calculate the real-time OMI from reforecast datasets. They also showed that the S2S models exhibit

prediction skill, measured by the bivariate correlation coefficient exceeding 0.6, ranging from ~15 to ~ 36 days in boreal winter. This is 5-10 days higher than the MJO circulation prediction skill based on the MJO RMM index, and the ROMI skill is systematically lower by 5 to 10 days in boreal summer than in winter. Interested readers may consult that paper for further details.

2.4 A linear regression model for the MJO index

In addition to the S2S models, we adopt a simple statistical model to help understand the MJO-QBO relation in a model in which any QBO influence is only – at most - implicit via the MJO state. A linear lag-regression model is written in standard form as:

$$\boldsymbol{y} = \boldsymbol{X\beta} + \varepsilon,$$

where the predictand variables are $\boldsymbol{y}$=[ROMI1(t+τ), ROMI2(t+τ)]$^{\mathrm{T}}$ with forecast initial date t and forecast lead $\boldsymbol{\tau}$. The predictors are ROMI values at the initial date t and the previous day, $\boldsymbol{X}$=[ROMI1(t), ROMI2(t), ROMI1(t-1), ROMI2(t-1), 1]$^{\mathrm{T}}$, and $\boldsymbol{\varepsilon}$ is random noise. The regression coefficient $\boldsymbol{\beta}$ is computed as a function of forecast lead τ using the ROMI data from 1979 to 2016. Importantly the regression coefficient does not vary with season or QBO phase. Jiang et al. (2008) and Kang and Kim (2010) showed that similar simple linear regression model exhibits the prediction skill for the MJO RMM index up to 15 days. This model will be referred to as the multiple linear regression (MLR) model throughout.

The MLR model is used to predict daily ROMI values during 1980 – 2016, with forecast lead times of 1 to 45 days and daily initialization to give the maximum possible

sample size. We compute the forecast correlation skill for the MJO events with initial amplitude greater than 1. The MLR forecasts are computed using regression coefficients that are estimated from all the data, since our intention is not to estimate the practical skill of the MLR model, but rather to use the MLR model to help understand the QBO-MJO connection in a forecast model that has no explicit QBO dependence.

3. Results

3.1 The QBO in the S2S models

The S2S models adopt distinct strategies for the initialization of the stratosphere, numerical schemes for gravity wave drag, and boundary conditions at the top of the atmosphere, all of which can potentially play important roles in maintaining the QBO circulation during the forecast periods. As a result, the QBO signatures in temperature and winds vary significantly across the S2S reforecasts. **Figure 1** shows the EQBO minus WQBO difference in boreal winter zonal mean zonal wind (ΔU) and zonal mean temperature (ΔT), averaged between 10°S and 10°N on 10 pressure levels from 1999 to 2010. The QBO zonal wind difference, ΔU, at 50 hPa in the S2S models ranges from -5 m/s to more than -20 m/s. The QBO temperature, ΔT, peaks at 100 hPa, and ranges from -0.3 K to -1 K. Negative values of ΔT extend down to the lower troposphere. BOM (gray) shows the smallest differences in both ΔU and ΔT, perhaps because it has the lowest model top (10 hPa). Further inspection of these variables indicates that the QBO signatures decrease faster with forecast leads in some models than others, as shown in Figures S1 and S2 of the supporting information.

3.2 Impact of QBO on MJO convection prediction and predictability in winter

187 The bivariate correlation skill (COR) in boreal winter (December to March) from
188 1999 to 2010, a common period of the S2S dataset, is computed for the 10 S2S models
189 as:

190 $$COR = \frac{\sum_i F_{1,i} O_{1,i} + F_{2,i} O_{2,i}}{\sqrt{\sum_i F_{1,i}{}^2 + F_{2,i}{}^2} \sqrt{\sum_i O_{1,i}{}^2 + O_{2,i}{}^2}}$$

191 where *i* denotes the index of the (re)forecasts, F1 and F2 denote the ROMI1 and ROMI2
192 from the reforecasts, respectively, and O1 and O2 are ROMI1 and ROMI2 derived from
193 observation. Model forecasts of the QBO are not used here, but will be tested in the next
194 section. **Figure 2a** shows the correlation skill, using COR = 0.5 and 0.6 as threshold
195 values, for all the S2S models in the two different QBO phases. The 10 S2S models
196 unanimously show higher prediction skill in winter during EQBO; for example, the
197 COR=0.5 difference is ~ 10 days in the ECMWF and NCEP models. On average, the
198 prediction skill difference between EQBO and WQBO is 10 days for COR=0.5 and 9
199 days for COR=0.6 (Fig. 2b). There is no obvious relation between the ROMI prediction
200 skill and prediction skill difference between WQBO and EQBO. Hence the quantitative
201 influence of the QBO appears to be independent of the MJO prediction in these S2S
202 models.

203 Marshall et al. (2017) showed that for similar initial MJO amplitudes, the
204 difference in the MJO RMM prediction skill between the two QBO phases in the BOM
205 forecasts is unchanged for the reforecasts from the BOM model, but they were unable to
206 rule out the influence of initial amplitude. On the other hand, it is possible that the MJO
207 prediction skill may be sensitive to the amplitude of the forecast target at various lead
208 times. We first test the initial amplitude dependence. **Figure 3 a and b** show the ROMI
209 correlation skill for the observed ROMI amplitude falling in the range 1.0-1.8 and >1.8

for two S2S models: ECMWF and NCEP, which yield relatively large sample size (~ 200-400). The ROMI correlation skill differs significantly in the two QBO phases for the two ranges. The difference in the prediction skill with initial amplitude 1.0-1.8 (solid curves) and stronger initial amplitude (>1.8) is weak, and marginal at best. We further test this dependence on the amplitude of ROMI at various forecast lead times: 0, 2, 4, …, 24 days for the S2S models. **Figure 3 c and d** show the ROMI correlation skill for the observed ROMI amplitude within the range 1.0-1.8 for ECMWF and NCEP. The ROMI correlation skill differs significantly in the two QBO phases regardless of initial or target amplitude. Other S2S models show similar contrasts despite smaller sample sizes (<100). These results indicate that the amplitude of the ROMI does not play a role in the ROMI's prediction skill dependence on the QBO phases.

We further examine the predictability of the MJO in these ensemble prediction systems under different QBO phases using the quantity $T|_{SNR=1}$, which is defined to be the time at which the signal and noise variances are equal. The bivariate signal to noise ratio (*SNR*) is written as the ratio between the variance of the ensemble mean forecast and total variance:

$$SNR(\tau) = \frac{\sigma_s^2}{\sigma_n^2}$$

The signal and noise of the ensemble forecasts are estimated as:

$$\hat{\sigma}_s^2 = \frac{1}{N-1}\sum_{n=1}^{N}\sum_{p=1}^{2}\left(\overline{X}_p^n - \overline{X}_p\right)^2,$$

$$\hat{\sigma}_n^2 = \frac{1}{N(E-1)}\sum_{n=1}^{N}\sum_{m=1}^{E}\sum_{p=1}^{2}\left(X_p^{nm} - \overline{X}_p^n\right)^2.$$

X_p denotes the OMI index, and the subscript p indicates its 2 principle components. N and E denote the number of forecasts and number of ensemble members, respectively. $\overline{X}$ is the overall mean, and $\overline{X}_p^n$ denotes ensemble mean.

SNR does not decrease to 1 by the end of their forecast in several models (NCEP, JMA, ECCC) due to under-dispersiveness. **Figure 4a** shows $T|_{SNR=1}$ for the remaining six ensemble prediction models. All these models show higher predictability for MJO-EQBO during winter, consistent with our analysis of COR. Specifically, $T|_{SNR=1}$ in the six models is consistently larger for MJO-EQBO than in MJO-WQBO by 1-11 days, depending on the model. BOM shows the largest difference (11 days), ECMWF shows a difference of 7 days, while the difference for UKMO is 1 day. As with prediction skill, there appears to be no relationship between the MJO predictability and its dependence on the QBO. **Figure 4b** indicates that the increase in predictability in EQBO may be attributed to higher $\hat{\sigma}_s^2$ (solid), since $\hat{\sigma}_n^2$ (dashed) shows no appreciable change in the two QBO phases.

Another measure of predictability closely related to the signal-to-noise ratio above for ensemble prediction is potential predictability, which takes one of the ensemble members as the truth, assuming the forecast model is perfect, and validates forecasts against it. **Figure 5**a shows that potential predictability in EQBO is notably higher than in WQBO in 8 out of 9 S2S ensemble models (excluding ISAC, which has one member), although the difference between the two QBO phases is quantitatively smaller than that in prediction skill (c.f. **Fig. 2**). With these metrics, we can re-examine the initial amplitude dependence; here we do so by selecting reforecast cases with the same initial amplitude range (1.0-1.6) in the ECMWF model. Here the initial amplitude is calculated from the

253 forecast ensemble member chosen for verification (not from observation as elsewhere).
254 **Figure 5** b shows that for the similar initial amplitude, MJO-EQBO on average maintains
255 stronger amplitude than MJO-WQBO for all the time leads in both forecasts and
256 observations, and the potential predictability (**Fig. 5c**) is notably higher. The MJO-
257 WQBO cases weaken more than in the MJO-EQBO cases at longer leads in this model,
258 which likely causes decreased skill of MJO-WQBO but is accounted for in potential
259 predictability. To further test initial amplitude dependence, we select the WQBO cases
260 with slightly higher amplitude range (1.1-1.7), as the initial amplitude is more
261 comparable between MJO-EQBO with initial amplitude (1.0-1.6) and MJO-WQBO (1.1-
262 1.7). Nevertheless, the potential predictability does not improve in MJO-WQBO; this
263 indicates that we may rule out the initial amplitude influence on the potential
264 predictability.

265 **3.3 Stratospheric conditions versus initial conditions/persistence**

266 Having established that the QBO state is strongly associated with variations in the
267 skill of MJO prediction in the S2S models, one may ask if the QBO state predicted by
268 each model is truly a causal factor influencing MJO prediction skill in that model. An
269 alternative hypothesis would be that the QBO influence is simply a consequence of the
270 initial conditions, since those are taken from observations in which the QBO-MJO
271 relationship is already present. Another alternative hypothesis would be that the MJO is
272 more inherently predictable – for example, more auto-correlated with itself over time – in
273 EQBO than WQBO years, so that even if there were no difference in the model forecasts
274 between QBO phases, they could show greater skill in EQBO than WQBO because they
275 are being compared to more predictable observations in EQBO.

The S2S models rely on both boundary conditions and initial conditions to make informative and skillful forecasts. The lower stratosphere, though not a boundary condition per se, may in some sense to function as one from the perspective of tropospheric weather. The S2S forecast models have very different lower stratosphere characteristics due to variations in numerics and physics (**Table 1**). The majority of the models have relatively high model tops, but 3 of the 10 models (BOM, ISAC, and HMCR,) have model tops at 5 hPa or lower (in altitude; higher in pressure). The high-top models have slightly higher mean MJO prediction skill difference (~12 days) than the low top models (~10 days) in winter (**Figure 2b**). To further explore the QBO's influence on MJO skill, one may attempt to correlate models' skill difference during EQBO and WQBO with various QBO signatures, for example, temperature or temperature stratification at 100 hPa, which seems to be a likely physical pathway for the MJO-QBO connection (e.g., Son et al. 2017; Martin et al. 2019; Densmore et al. 2019). However, we find that such analysis does not yield any statistically significant relationship, perhaps unsurprisingly given that the sample size is less than 10 (see Figure S4 in the supplemental information). This suggests that the model-predicted QBO has a weak influence on MJO prediction skill.

On the other hand, one may argue that, if the influence of the predicted QBO state on MJO evolution is maintained in each model through the forecast – as opposed to entering only through the initial conditions – then the difference in noise estimates ($\hat{\sigma}_n^2$) between the two QBO phases should be significant. However, as shown in **Fig. 3b** this is not the case: instead, the difference in the signal estimates ($\hat{\sigma}_s^2$) in two QBO phases is robust across the S2S models, suggesting that the difference in prediction skill and

299 predictability shown above comes from the initial conditions or persistence. In the
300 following, we will present further evidence supporting this hypothesis.

301 **Figure 6** a, d, g show the lag correlation between the two principal component
302 time series (PC1 and PC2) for three MJO indices: RMM, OMI, and ROMI. All indices
303 have higher peak values around day 10 in EQBO than in WQBO. The period implied by
304 the days between the maximum value at positive leads and the minimum at the negative
305 leads is also longer in EQBO than in WQBO by a few days.

306 We next examine the mean phase angle Θ, defined as:

307 $$\Theta = arctan\left(\frac{1}{N}\sum_i \sin\theta_i\ , \frac{1}{N}\sum_i \cos\theta_i\right),$$

308 where θ is the phase angle between the PC1 and PC2 components of the ROMI index.
309 The composites of the mean phase angle (Wang et al. 2018 a,b) in EQBO and WQBO in
310 the middle and right columns of **Figure 6** further break down the phase propagation into
311 8 phases. The mean phase angle is noisier in MJO-WQBO than in MJO-EQBO,
312 propagating with near constant phase speed in the latter. The lag correlation and phase
313 composite together indicate that the observed MJO indices in EQBO are inherently more
314 regular and less noisy than in WQBO, consistent with the greater predictability in EQBO
315 shown above.

316 The difference in the MJO indices as shown above reflects changes in the MJO's
317 dynamical structures in the two QBO phases. To illustrate this point, we composite the
318 reconstructed OLR from the OMI index upon the QBO. The MJO events are searched
319 forward from 1979 to 2016, based on the following criteria: (1) OMI is in phase 3 or 4 at
320 day 0 such that the convection is located around Maritime Continent; (2) the OMI
321 amplitude is greater than 0.5 at day 0; (3) any two selected events must be separated by at

least 30 days to prevent double-counting. Using the same QBO index and criteria (-2.37 and 5.23 m/s) for QBO phases, this leads to 29 MJO-EQBO events, and 31 MJO-EQBO events in 1979-2016. The results described below is not sensitive to the period. The reconstructed OLR anomalies *R* are computed as:

$$R(x,y,t) = \mathrm{PC1}(t)\times\mathrm{EOF1}(x,y,doy) + \mathrm{PC1}(t)\times\mathrm{EOF1}(x,y,doy),$$

where PCs are the principle component time series, EOFs are the empirical orthogonal functions, and *doy* denotes day-of-year.

Figure 7 shows the lag composites of the reconstructed OLR and zonal wind at 850 hPa (U8) anomalies in the two QBO phases. The MJO OLR anomalies are notably stronger in EQBO (**Fig. 7a**) than in WQBO (**Fig. 7b**). The period at 100 °E is ~ 5-10 days longer in EQBO than in EQBO in both OLR and U8. Correspondingly, the phase speed of MJO-EQBO is notably slower, as also alluded in Figure 3 of Zhang and Zhang (2017) for precipitation. The structural difference is robust in 850 hPa zonal wind (**Fig. 7 c and d**), and also in different MJO phases at day 0 or if different indices are used (not shown). This illustrates that the MJO-EQBO and MJO–WQBO are within different spectra of the broad intraseasonal band: MJO-EQBO is stronger, propagates slower, and has longer period than MJO-WQBO.

Now we proceed to analyze the structural difference between the MJO-EQBO and MJO–WQBO in reforecasts. Similar to the composite analysis for observation in **Fig. 7**, right panels of **Figure 8** shows that the reconstructed OLR anomalies from the predicted ROMI initialized at phase 3-4 with initial amplitude greater than 1 for the ECMWF and NCEP models. The verifications differ for each model because of difference in the initialization times, and are also shown in the left panels. As **Fig. 7**, the verifications in

345 the two models show MJO-EQBO is slower and stronger than MJO-WQBO. The MJO-
346 EQBO in forecasts is slower and stronger, and comparable to verification except for the
347 bias at longer leads. But MJO-WQBO (**Fig. 7** d and h) in forecasts is notably slower than
348 verification, which might contribute to the skill reduction in WQBO. The contrast
349 between the two is weaker in forecasts than in observations. This suggests that potential
350 predictability, which takes one ensemble member of forecasts for validation (**Fig. 3**),
351 should also display difference between MJO-EQBO and MJO-WQBO. Indeed, this is
352 what was demonstrated in **Fig. 4**. The structural difference between MJO-EQBO and
353 MJO-EQBO in reforecasts can also be identified from the ROMI values. The correlation
354 between ROMI1 and ROMI2 in forecasts for all the models (Fig. S5 in the supporting
355 information) shows higher peak values in MJO-EQBO than in MJO-WQBO.
356 Next, we test the influence of the QBO in the MLR model. We compute the
357 correlation between the MLR-predicted ROMI values and the observations in the same
358 manner as we computed that between the S2S reforecasts and observations. **Figure 9**
359 shows that the MLR prediction skill in EQBO and WQBO differ by more than 10 days
360 using the threshold COR=0.5; this is true both from 1999-2010 (**Fig. 9b**), and similarly
361 during 1979 - 1999 (**Fig. 9a**). This large difference is quantitatively consistent with the
362 S2S model results (**Fig. 2b**). However, as discussed in **Section 2.4**, the MLR coefficients
363 are independent of the QBO phase. The MLR model prediction is based only on the state
364 of MJO on the initial and previous days, and uses no explicit information about the state
365 of the stratosphere (or anything else other than the OMI index). As a result, the MLR
366 model is agnostic to the explicit QBO phase. Despite this, the fact that MLR still captures
367 the QBO influence on the MJO prediction skill indicates that the QBO influence is

368 implicitly included in the initial conditions of the MLR model and in the verifying
369 observations. The results also confirm Marshall et al.'s (2017) finding that the influence
370 of the stratosphere on the MJO prediction is robust in a statistical model without explicit
371 knowledge of stratosphere.

372 Taken together, our results lead us to several inferences. First the MJO prediction
373 is strongly dependent on the observed QBO state, but weakly dependent on the QBO
374 state in the S2S forecasts. Second, the EQBO-WQBO differences in both potential
375 predictability and signal-to-noise ratio indicates that differences in MJO persistence in
376 the target observations cannot be the sole factor responsible for the differences in real
377 prediction skill, since the target observations are not used in computing these measures.
378 Third, the observed MJO index is less noisy and more regular in EQBO, and the MLR
379 shows better skill during EQBO, even though it contains no information about the
380 stratosphere; these facts suggest that, the previous inference notwithstanding, increased
381 persistence in the tropospheric MJO during EQBO vs. WQBO is at least part of the
382 explanation for the increased actual prediction skill in EQBO vs. WQBO.

383 These inferences collectively lead us to the broader conclusion that differences in
384 the forecast QBO in the models are not the main factor contributing to the MJO skill
385 difference between EQBO and WQBO. Rather, EQBO-WQBO differences in both initial
386 conditions and the target observations used for verification appear to play roles. The
387 relevant differences in initial conditions, however, cannot simply be differences in
388 amplitude, since controlling for amplitude does not eliminate the differences in prediction
389 skill. What structural differences in the MJO are important and how those are manifest in
390 the initial conditions is a topic for future research.

3.4 Impact of QBO on BSISO prediction skill in boreal summer

The above discussion focuses on the QBO influence on MJO predictions in boreal winter. We explore this relation for the boreal summer intraseasonal oscillation (BSISO). **Figures 10 a and b** show COR in boreal summer (June - September) during 1999-2010. In many S2S models, COR is higher by ~ 10 days under WQBO than EQBO using either COR =0.5 or 0.6 as a threshold. This is in stark contrast with the QBO-MJO prediction in winter. This strong QBO influence on MJO prediction and predictability in summer is unexpected. Yoo and Son (2016) showed that there is there is no linear correlation between QBO and MJO-OMI amplitude in summer, in contrast to winter. However, most S2S models only have limited reforecast periods, and here they are compared over the common period in 1999 – 2010. As will be discussed below, a consistent relation between QBO and MJO-OMI amplitude in summer is indeed present in observations during this period.

To examine this relationship further, we composite the OMI reconstructed OLR anomalies on the QBO phases in boreal summer (May to October) in the recent four decades: 1980 – 1990, 1990-2000, 2000-2010, 2010-2016. **Figure 11** shows the variances of the reconstructed OLR anomalies in WQBO, EQBO and the difference between these two QBO phases. The maximum variances are located over the eastern equatorial Indian Ocean, Bay of Bengal, South China Sea, and northwest Western tropical Pacific Ocean in both QBO phases. These patterns are consistent with those found in prior studies (e.g., Lawrence and Webster 2002, Sobel et al. 2010). The difference in OLR intraseasonal variance between the two QBO phases is shown in the

414 rightmost column of **Figure 11** for each of the past four decades. The variance under
415 EQBO (leftmost column) does not seem to have any strong decadal variations during the
416 past 4 decades. However, the variance in WQBO (middle column) is particularly strong
417 in 2000-2010, compared to the other decades. The difference in variance (indicated by
418 hatching) is statistically significant at the 95% level in most areas using Levene's test
419 (Levene 1960). Hence, the QBO influence on intraseasonal convection is at times
420 reversed in the boreal summer: the BSISO convection is reduced in EQBO in 2000-2010,
421 in contrast to its strengthening in the other three decades. A similar composite analysis
422 was also performed for boreal winter, and in that case we do not see a change in the
423 QBO-MJO relationship from one decade to the next since 1979.

424 The above composite strongly suggests that the QBO influence on ROMI
425 prediction skill during summer should also exhibit decadal variability. However, this is
426 difficult to evaluate using the S2S models, as most of the S2S models have limited
427 reforecast periods that do not extend back to 1980. To further explore this hypothesis, we
428 examine the QBO influence on BSISO prediction using the MLR model. The MLR
429 correlation skill is estimated during two different periods, 1979-1999 and 1999-2010, to
430 examine QBO influences on the BSISO prediction skill over these time periods of
431 interests.

432 **Figure 12** shows that this simple statistical model has skill extending to 19 days
433 using the threshold bivariate correlation = 0.5. This skill is lower than that of most S2S
434 models in summer (**Fig. 12**). We calculate the COR for 2 periods: 1979 to 2016, and
435 1999 to 2010. **Figures 12** a and b show that the summer COR from the MLR model is
436 higher under WQBO during 1999 to 2010, similar to the S2S models (**Fig. 10 b**). But this

relationship reverses during 1979 to 2000. The opposite impact QBO on summer bivariate correlation skill is also consistent with the composite of the OLR anomalies discussed above.

4. Conclusions

We have examined the impact of the stratospheric quasi-biennial oscillation (QBO) on the prediction skill of tropical intraseasonal convection represented by the real-time OLR MJO index (ROMI) in the WMO Subseasonal to Seasonal forecast models. While some S2S models do not have well-resolved stratospheres because of relatively low model tops, the stratospheric QBO nevertheless has a strong relationship with ROMI prediction skill across the ensemble of S2S models. The skill during boreal winter is higher in the QBO easterly phase (EQBO) in all 10 models by ~10 days, using the anomaly correlation coefficient 0.5 as a criterion during 1999-2010; this relation is independent of the MJO prediction skill in the individual models, across the ensemble. In contrast, the skill in boreal summer decreases in EQBO during this period. It is further shown that there is also a close relationship between the QBO and BSISO, but that this relationship varies over the past several decades, with a stronger BSISO during the QBO westerly phase during the 1st decade of the 21th century and a stronger BSISO under EQBO during other periods.

Analysis of the observations indicates that during winter, several different MJO indices (OMI, ROMI, RMM) are inherently less noisy and hence more predictable in EQBO. Potential predictability analysis shows qualitatively similar but smaller contrast between the two QBO phases, indicating that the QBO dependence of actual prediction

skill is not solely due to the verifying observations. Compositing the MJO OLR anomalies upon QBO shows that the MJO-EQBO is stronger, has a longer period, and propagates more slowly. Further, a simple regression model has higher skill during EQBO than during WQBO, even though it does not contain any explicit information about the stratosphere.

Taken together, these results suggest that the relationship between QBO phase and MJO prediction skill in northern winter is a consequence of EQBO-WQBO differences in the initial conditions (though not solely in amplitude), in the persistence of the MJO in the verifying observations, or – most likely - some combination of the two, but not of an actual stratospheric influence exerted on the tropospheric MJO within the model simulations.

While our analysis strongly suggests that the stratosphere is not crucial for the prediction of the MJO under the influence of the QBO, our results do not disprove the general notion that stratosphere-troposphere coupling is important for tropospheric weather. In contrast, our analysis illustrates the added complexity in the predictability problems that involve initial conditions, forecast verification, and dynamical coupling between troposphere and other components of the earth systems, e.g., stratosphere, ocean and land.

Acknowledgement

This research has been conducted as part of the NOAA MAPP S2S Prediction Task Force and supported by NOAA grant NA16OAR4310076. SW and AHS also acknowledge support from NSF AGS-1543932 and ONR N00014-16-1-3073. We thank Haibo Liu for obtaining and organizing the S2S data set from the ECMWF data portal.

The S2S reforecast dataset is available at: http://apps.ecmwf.int/datasets/data/s2s-reforecasts-instantaneous-accum-ecmf/levtype=sfc/type=cf/, and https://iridl.ldeo.columbia.edu/SOURCES/.ECMWF/.S2S

The QBO index is available through http://www.cpc.ncep.noaa.gov/data/indices/qbo.u50.index

The ROMI index from 1979 to 2018 is available from the first author.

References

Baldwin, M.P.; Gray, L.J.; Dunkerton, T.J.; Hamilton, K.; Haynes, P.H.; Randel, W.J.; Holton, J.R.; Alexander, M.J.; Hirota, I.; Horinouchi, T.; Jones, D.B.A. (2001). "The quasi‐biennial oscillation". Rev. Geophys. 39 (2): 179–229.

Dee, D. P., et al. (2011), The ERA-Interim reanalysis: Configuration and performance of the data assimilation system, Q. J. R. Meteorol. Soc., 137(656), 553–597.

Densmore, C.R., E.R. Sanabia, and B.S. Barrett, 2019: QBO Influence on MJO Amplitude over the Maritime Continent: Physical Mechanisms and Seasonality. Mon. Wea. Rev., 147, 389–406, https://doi.org/10.1175/MWR-D-18-0158.1

Fisher, N. I. (1993): Statistical Analysis of Circular Data, Cambridge University Press, Cambridge, 277 pp.

Fraedrich, K., S. Pawson, and R. Wang (1993), An EOF analysis of the vertical-time delay structure of the quasi-biennial oscillation, J. Atmos. Sci., 50(20), 3357–3365.

Hendon, H. H., & Abhik, S. (2018). Differences in vertical structure of the Madden-Julian Oscillation associated with the quasi-biennial oscillation. Geophysical Research Letters, 45. https://doi.org/10.1029/2018GL077207

Lawrence, D.M. and P.J. Webster, 2002: The Boreal Summer Intraseasonal Oscillation: Relationship between Northward and Eastward Movement of Convection. J. Atmos. Sci., 59, 1593–1606, https://doi.org/10.1175/1520-0469(2002)059<1593:TBSIOR>2.0.CO;2

Levene, H. (1960). "Robust tests for equality of variances". In Ingram Olkin; Harold Hotelling; et al. Contributions to Probability and Statistics: Essays in Honor of Harold Hotelling. Stanford University Press. pp. 278–292.

Lee, J. Y., B. Wang, M. C. Wheeler, X. Fu, D. E. Waliser, and I.-S. Kang, 2013: Real-time multivariate indices for the boreal summer intraseasonal oscillation over the Asian summer monsoon region. Clim Dyn., 40, 493–509, doi:10.1007/s00382-012-1544-4.

Lee, J. C. K. and Klingaman, N. P. (2018) The effect of the Quasi-Biennial Oscillation on the Madden-Julian Oscillation in the Met Office Unified Model Global Ocean Mixed Layer configuration. Atmospheric Science Letters. DOI: 10.1002/asl.816

Li, T., L. Wang, M. Peng, B. Wang, C. Zhang, W. Lau, and H. Kuo, 2018: A Paper on the Tropical Intraseasonal Oscillation Published in 1963 in a Chinese Journal. Bull. Amer. Meteor. Soc. doi:10.1175/BAMS-D-17-0216.1, in press.

Martin, Z., S. Wang, J. Nie, A. H. Sobel, 2018. The influence of the quasi-biennial oscillation on the Madden-Julian oscillation in idealized cloud-resolving. J. Atmos. Sci., In review.

Marshall, A. G., H. H. Hendon, S.-W. Son, and Y. Lim, 2017: Impact of the quasi-biennial oscillation on predictability of the Madden–Julian oscillation. Clim. Dyn., 49: 1365. https://doi.org/10.1007/s00382-016-3392-0

Nishimoto, E., and S. Yoden, 2017: Influence of the stratospheric quasi-biennial oscillation on the Madden–Julian oscillation during austral summer. J. Atmos. Sci., 74, 1105–1125, https://doi.org/10.1175/JAS-D-16-0205.1

Solomon, A., J. H. Richter, and J. T. Bacmeister (2014), An objective analysis of the QBO in ERA-Interim and the Community Atmosphere Model, version 5, Geophys. Res. Lett., 41, 7791–7798, doi:10.1002/2014GL061801.

Son, S.-W., Y. Lim, C. Yoo, H. H. Hendon, and J. Kim, 2017: Stratospheric control of Madden–Julian oscillation. J. Climate, 30, 1909–1922, doi:https://doi.org/10.1175/JCLI-D-16-0620.1.

Vitart, F. (2017), Madden—Julian Oscillation prediction and teleconnections in the S2S database. Q.J.R. Meteorol. Soc, 143: 2210–2220. doi:10.1002/qj.3079

Wallace, J. M., R. L. Panetta, and J. Estberg (1993), Representation of the equatorial stratospheric quasi-biennial oscillation in EOF phase space, *J. Atmos. Sci.*, 50(12), 1751–1762.

Wang, S., D. Ma, A.H. Sobel, M.K. Tippett (2018a), Propagation characteristics of BSISO indices. Geophys. Res. Lett., 45. https://doi.org/10.1029/2018GL078321

Wang, S., A.H. Sobel, M.K. Tippett, F. Vitart (2018b), Prediction and predictability of tropical intraseasonal convection. Climate. Dynamics. In press.

Wheeler, M.C. and H.H. Hendon, 2004: An All-Season Real-Time Multivariate MJO Index: Development of an Index for Monitoring and Prediction. Mon. Wea. Rev., 132, 1917–1932,

Xie, Y.-B., S.-J. Chen, I-L. Zhang, and Y.-L. Hung, 1963: A preliminarily statistic and synoptic study about the basic currents over southeastern Asia and the initiation of typhoon. Acta Meteorologica Sinica, Vol. 33, No. 2, 206-217 (in Chinese).

Yoo, C., and S.-W. Son, 2016: Modulation of the boreal wintertime Madden–Julian oscillation by the stratospheric quasi-biennial oscillation. Geophys. Res. Lett., 43, 1392–1398, doi:https://doi.org/10.1002/2016GL067762.

Zhang, C., & Zhang, B. (2018). QBO-MJO connection. *Journal of Geophysical Research: Atmospheres*, 123, 2957–2967. https://doi.org/10.1002/2017JD028171

Table 1 S2S model configuration: horizontal and vertical resolution of atmosphere component, model top, reforecast types, forecast periods, reforecast frequency, and ensemble size. Reforecast types are either F (fixed), or O (on the fly). The CNR-ISAC model version is 20150326.

	Resolution	Model top	Rfc type	Rfc period	Rfc frequency	Ens size	O/A coupling
BOM	~ T47 L17	10 hPa	F	1981-2013	6 /month	3*11	Y
CMA	T106 L40	0.5 hPa	F	1994-2013	daily	4	Y
CNR-ISAC	0.75×0.56 L54	~6.8 hPa	F	1981-2010	every 5 days	1	slab
CNRM	T255L91	0.01 hPa	F	1993-2013	2 /month	15	Y
ECCC	0.45×0.45 L40	2 hPa	O	1995-2013	weekly	4	persistent SST
ECMWF	T639/319 L91	0.01 hPa	O	1996-2013 (past 20 years)	2 /week	11	Y
HMCR	1.1×1.4 L28	5 hPa	O	1985-2010	weekly	10	N
JMA	T319L60	0.1 hPa	F	1981-2010	3 /month	5	N
NCEP	T126L64	0.02 hPa	F	1999-2010	daily	4	Y
UKMO	N216L85	85 km	O	1996-2015	4 /month	3	Y

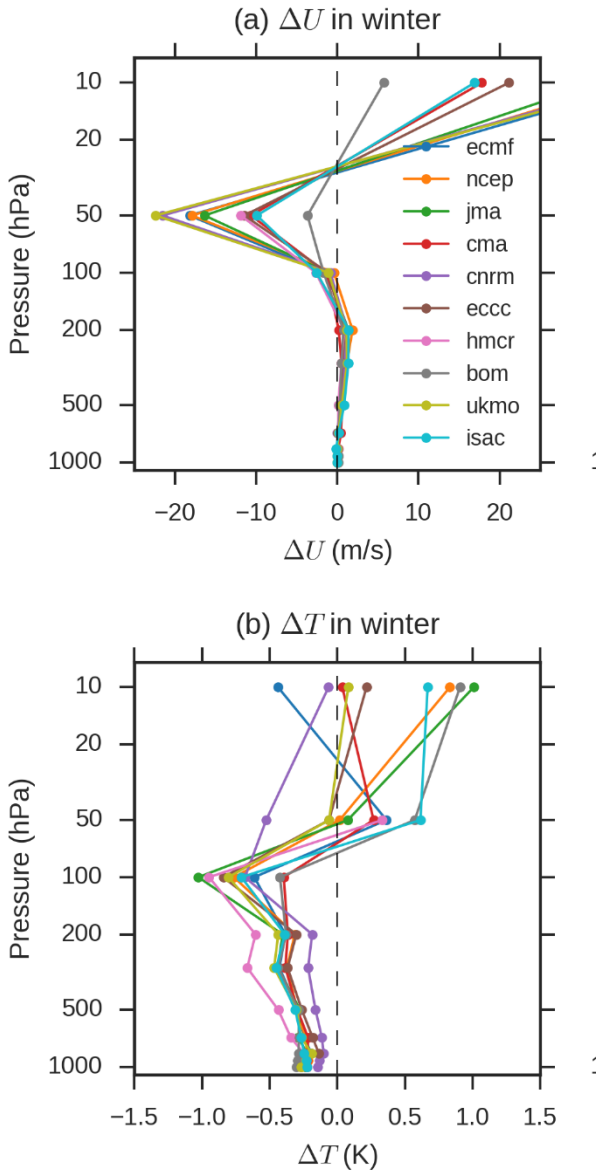

Figure 1. Top panel: composite of difference in tropical zonal mean zonal winds during in QBO easterly vs QBO westerly ΔU boreal winter during the first 30 days of the S2S models. Bottom panel: as top panel, but for zonal mean temperature.

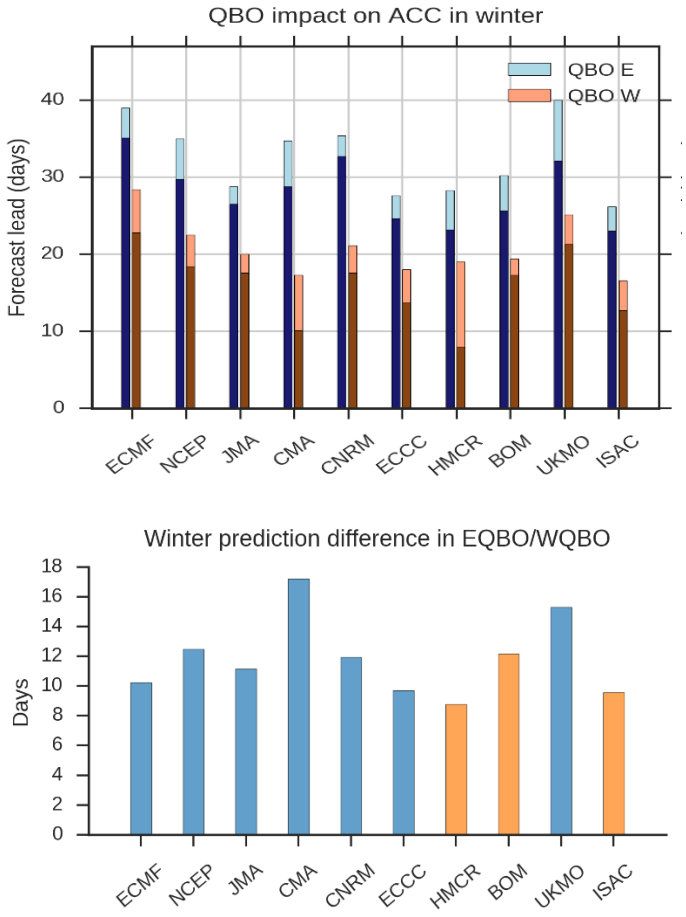

Figure 2. (a) Impact of QBO on the OMI prediction skills in winter using criteria ACC = 0.5 and 0.6 in boreal winter. (b) Difference in anomaly correlation skill between WQBO and EQBO in boreal winter 1999-2010. Blue: modes with higher top (< 5 hPa); yellow: models with lower model top (>= 5hPa).

(a)

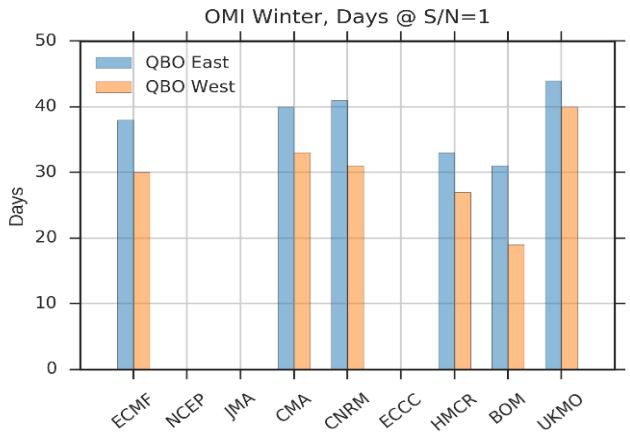

(b)

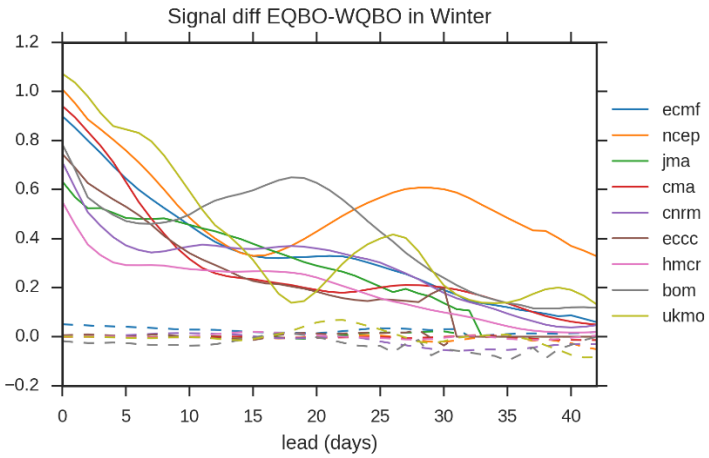

Figure 3. (a) Predibility measure using time when SNR (signal to noise ratio) = 1. (b) Difference in signal $\hat{\sigma}_s^2$ (solid) and noise $\hat{\sigma}_n^2$ (dashed) between EQBO and WQBO.

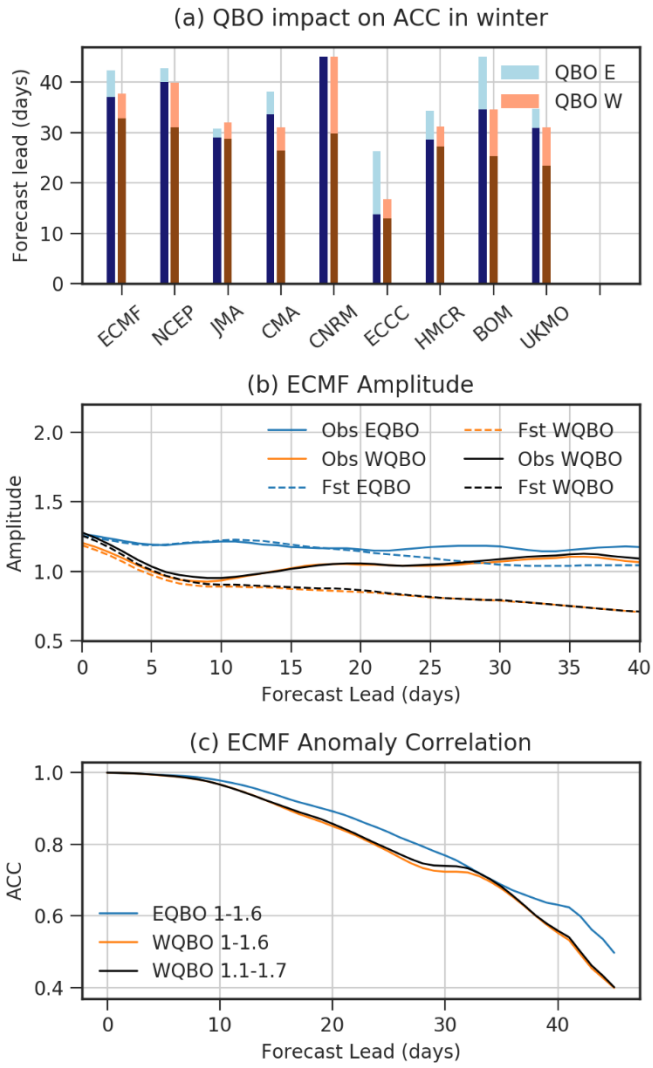

Figure 4. (a) Potential predictability. (b) Composite of amplitude in observation (solid) and reforecasts (dashed) from ECMWF with initial amplitude within the range 1-1.6 for EQBO and WQBO, and for WQBO (1.1-1.7). (c) Correlation skill for ECMWF for EQBO (1-1.6), WQBO (1-1.6), and WQBO (1.1-1.7).

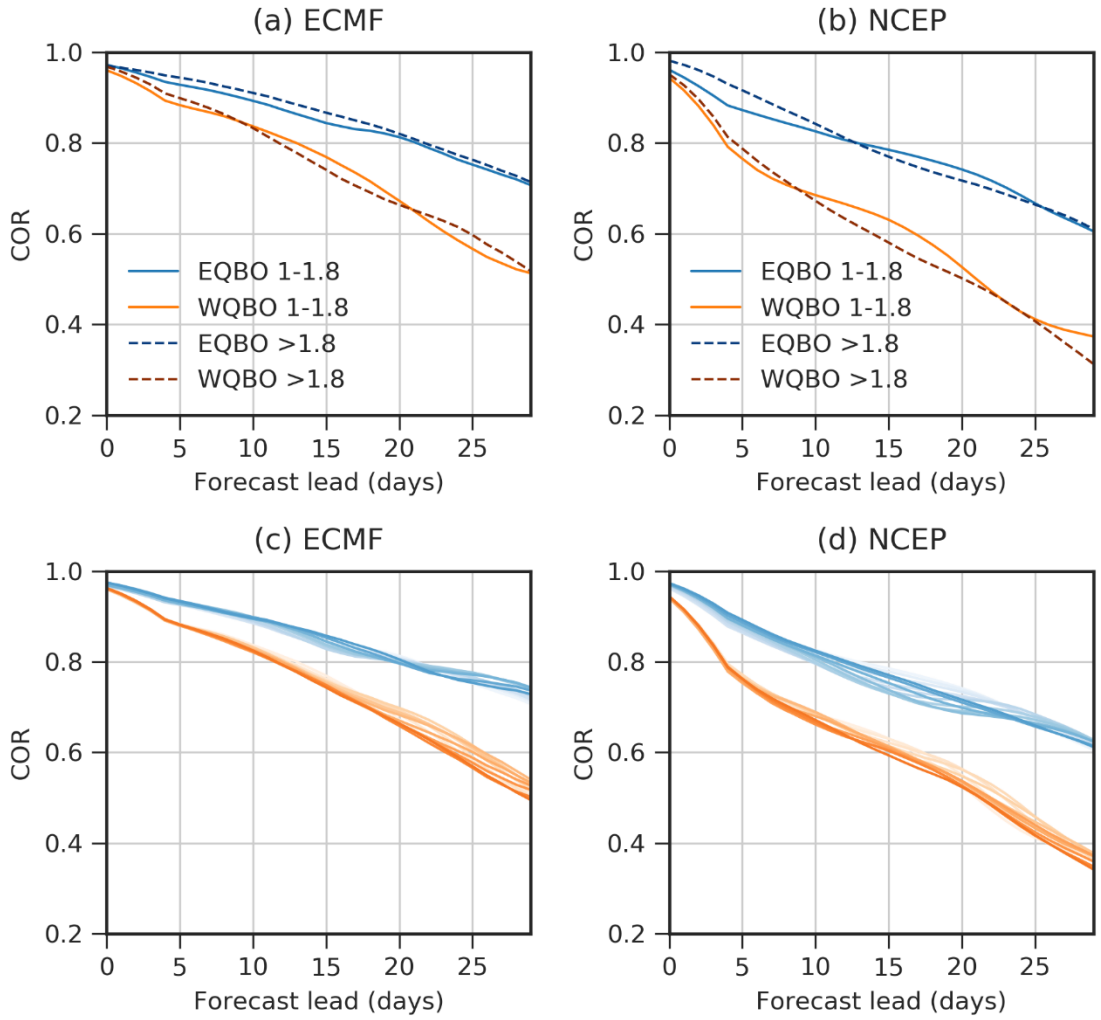

Figure 5. Top panels: Correlation skill for the reforecasts with initial amplitude falling into the range 1.0-1.8 (solid) and >1.8 (dashed) in the EQBO (blue) and WQBO (orange) for (a) ECMWF and (b) NCEP. Bottom panels: as top, but for the initial/target amplitude range in the range 1.0-1.8 for (c) ECMWF) and (d) NCEP. Individual curve denotes the composite for the amplitude at various forecast lead days: 0, 2, 4, …, 24. Light colors indicate small lead day composite; dark colors, longer lead composite.

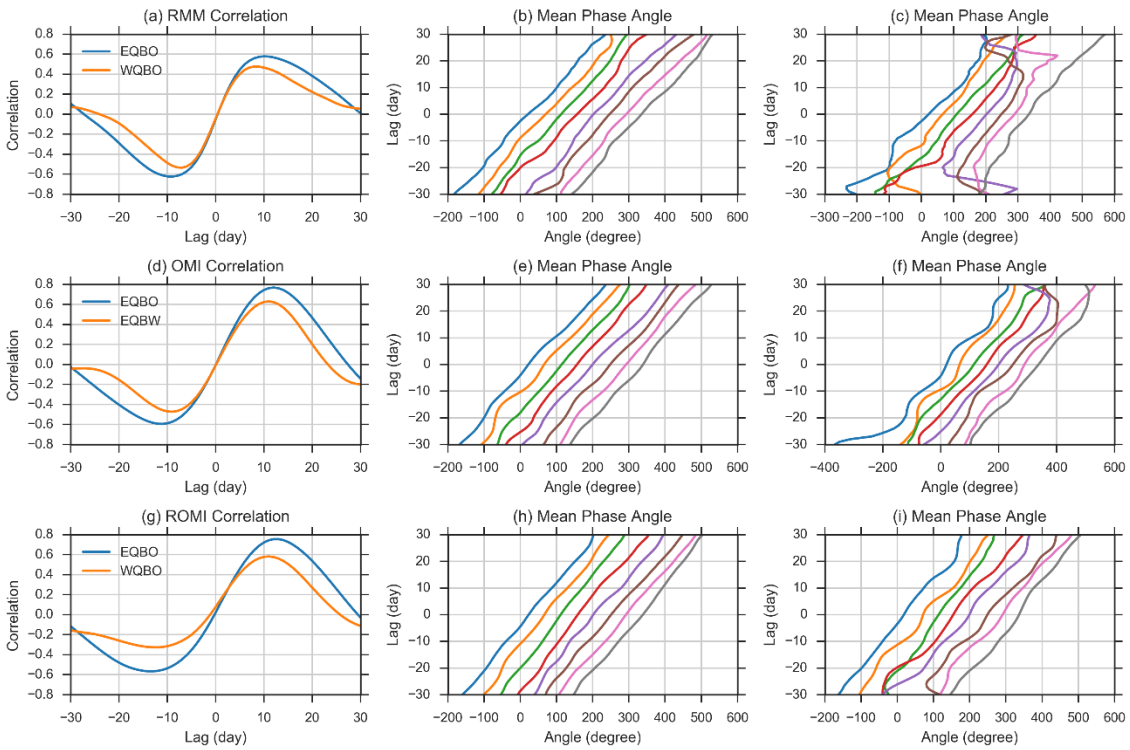

Figure 6. Top row: (a) correlations between PC1 and PC2 for RMM in EQBO and WQBO in boreal winter; (b) Composite of mean phase angles in EQBO; (c) as in (b) but in WQBO. Mid row, as top row but for OMI. Bottom row, as top row but for ROMI.

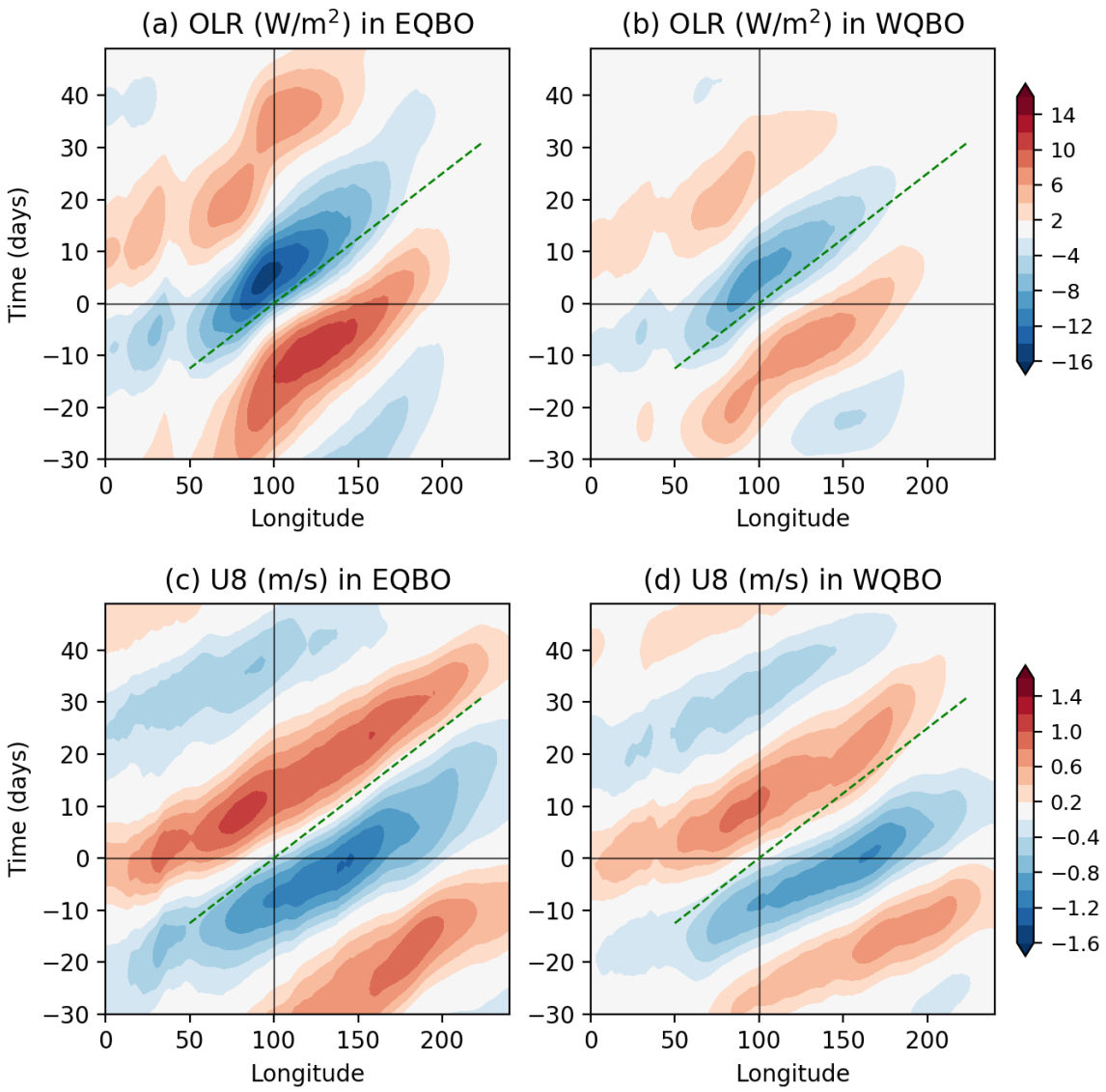

Figure 7. (a) Composite of OMI reconstructed OLR anomalies in EQBO; (b) as (a) but for WQBO. Green dashed lines indicate propagation speed 5 m/s.

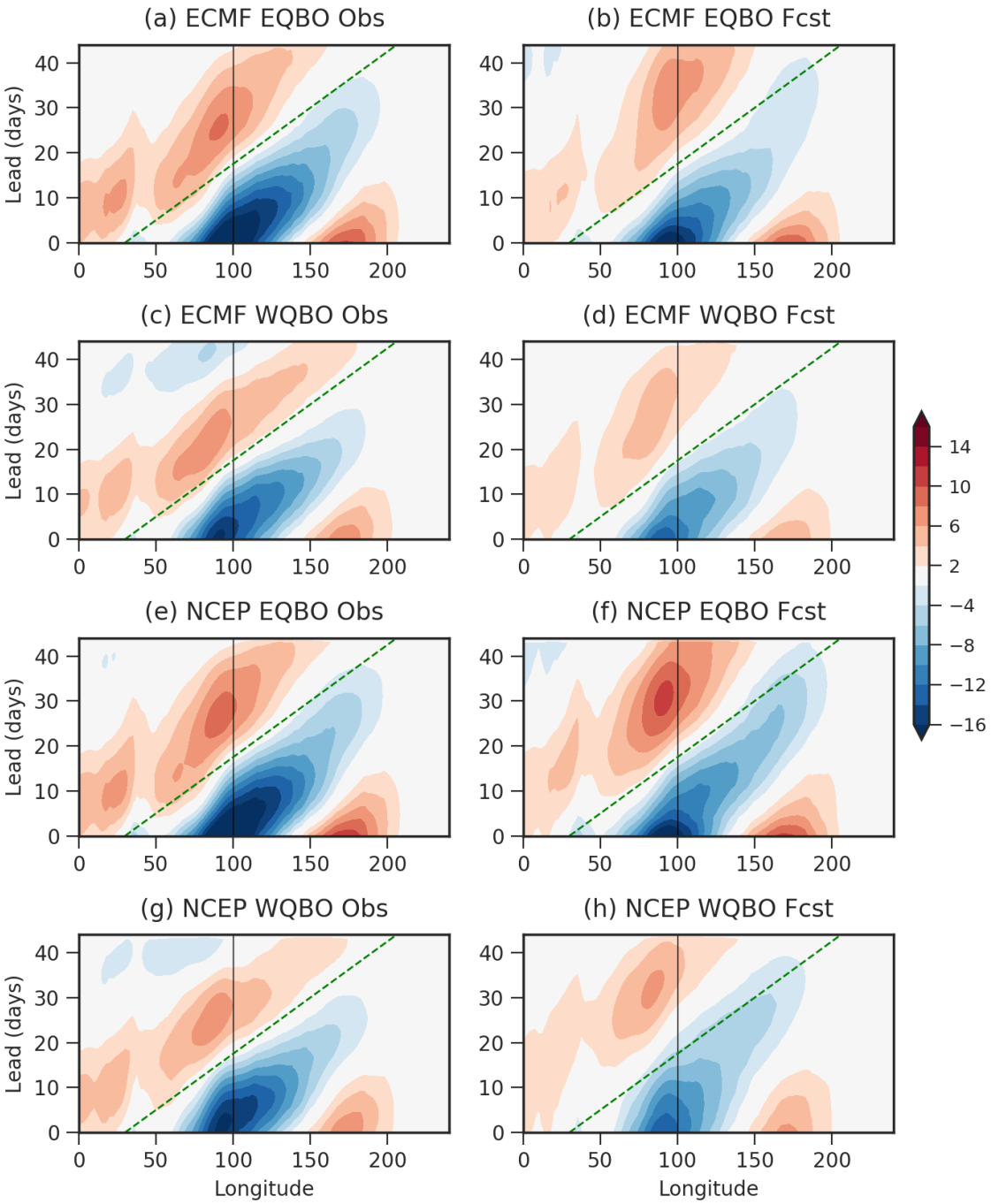

Figure 8. ROMI reconstructed OLR anomalies (W/m^2) averaged 20 °S-20 °N from ECMWF and NCEP models in EQBO and WQBO. Left panels: verification. Right panels: forecasts. Green dashed lines indicate propagation speed 5 m/s.

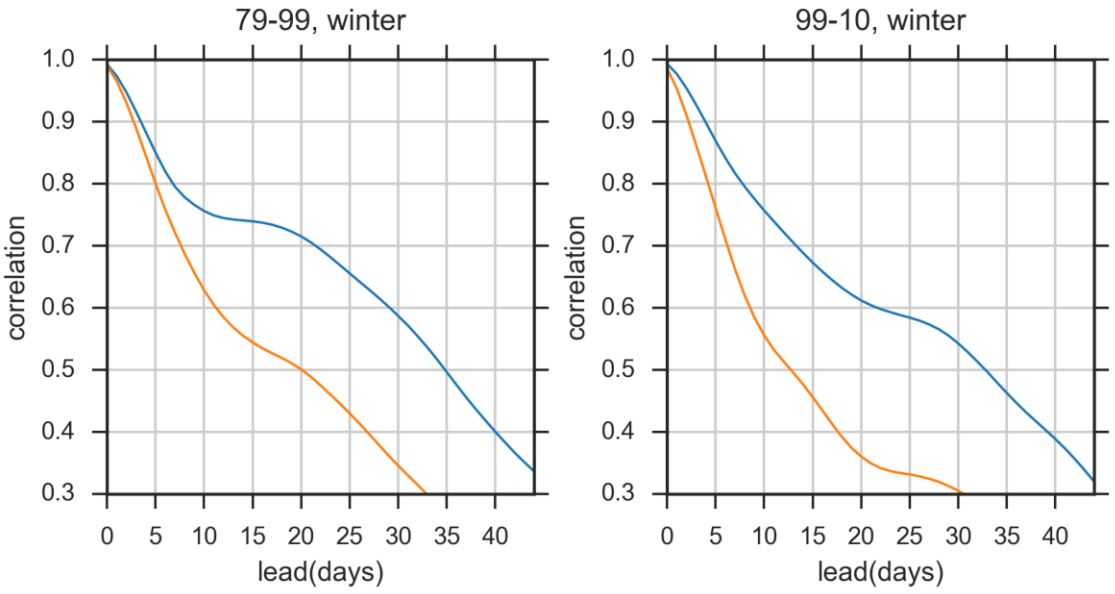

Figure 9. Correlation between the fitted PCs by the MLR and observation in boreal winter during 1979-1999 (a) in the left panel, and 1999-2010 (b) in the right panel, the common period for the S2S models. Blue curve: MJO-EQBO. Orange curve: MJO-WQBO.

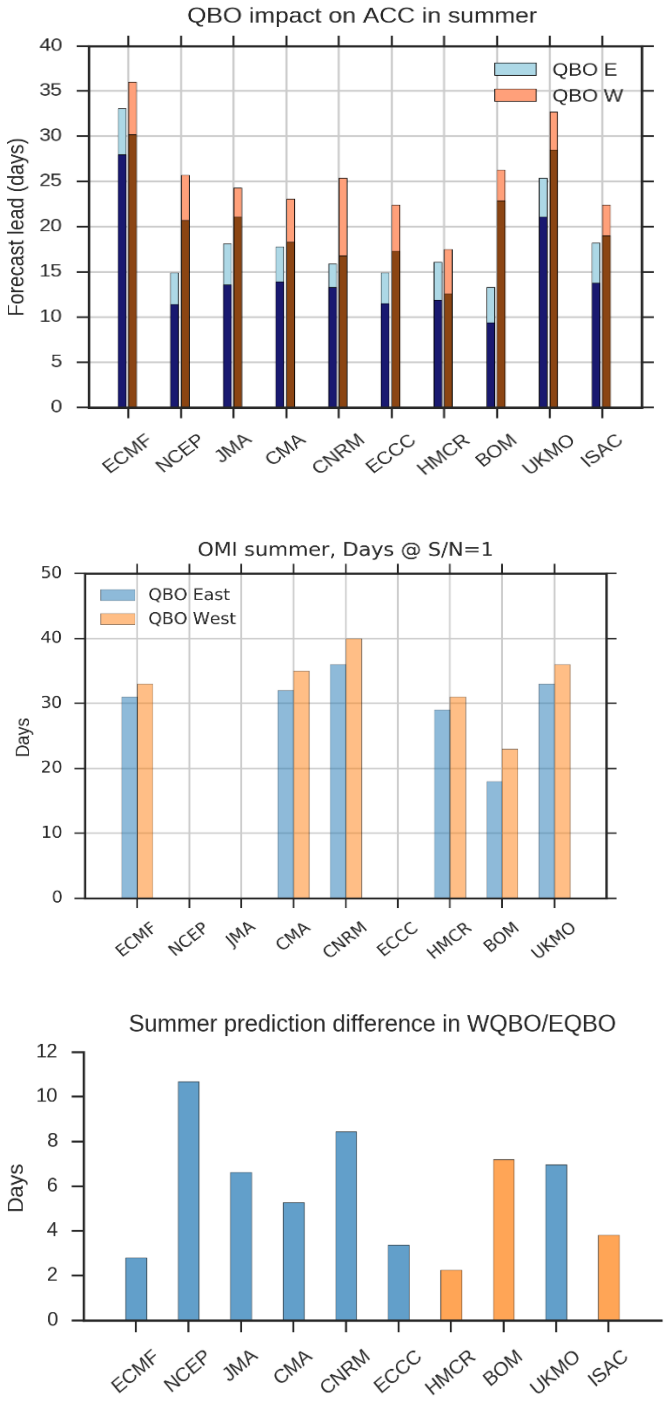

Figure 10. (a) Impact of QBO on the OMI prediction skills in winter using criteria ACC = 0.5 and 0.6 in boreal summer. (b) Predibility measure using time when SNR (signal to noise ratio) = 1. (c) Difference in anomaly correlation skill between WQBO and EQBO in boreal summer 1999-2010. Blue: modes with higher top (< 5 hPa); yellow: models with lower model top (>= 5hPa).

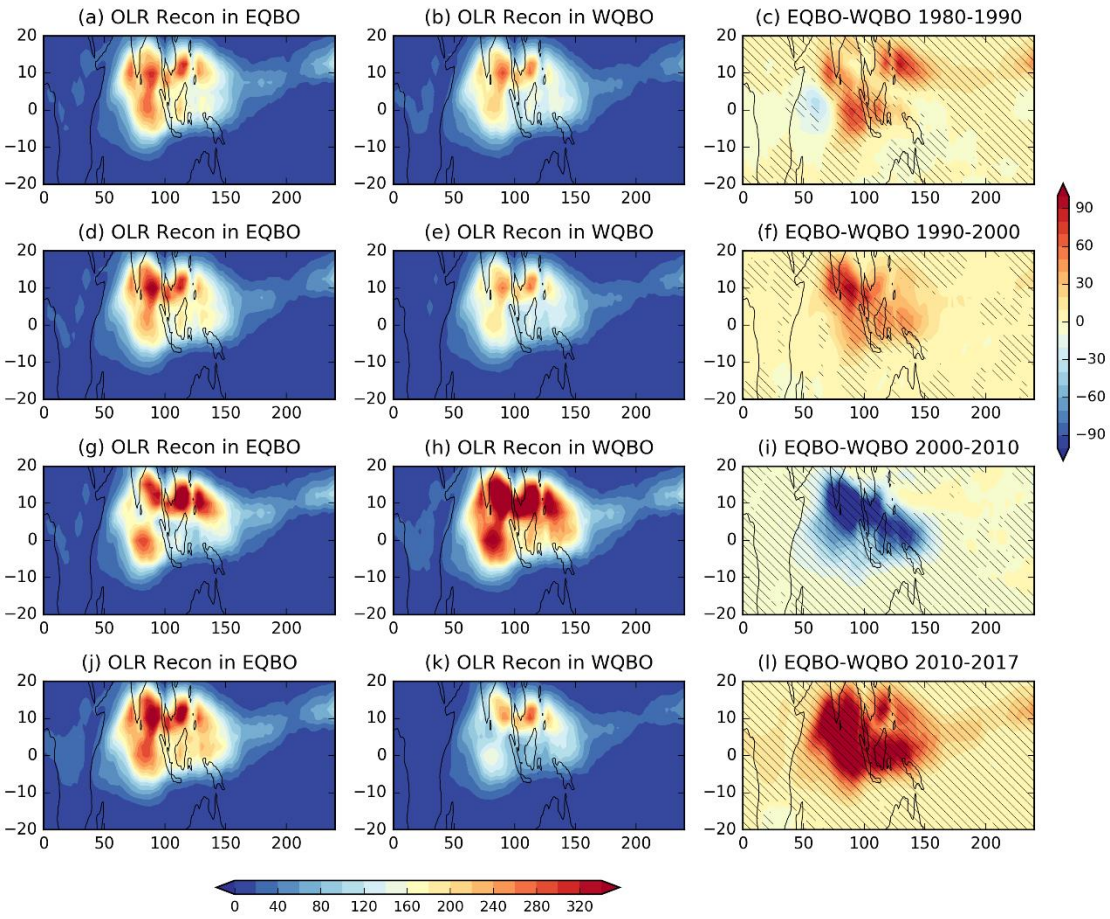

Figure 11. Variance of reconstructed OLR anomalies (W^2/m^4) from the OMI index in the summer season (July to September) in 4 decades under QBO easterly (left column) and westerly (middle column) phases, and the difference in the 2 QBO phases (rightmost column). Hatches in the rightmost columns indicate the difference in variances are statistically significant at 95% percent level from Levene's test.

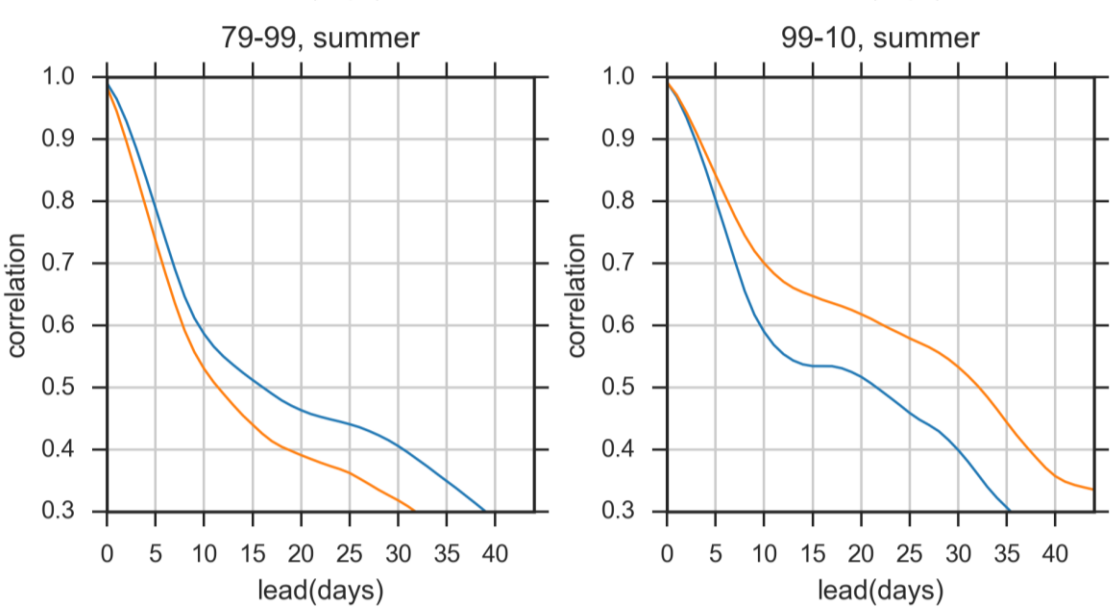

Figure 12. Correlation between the fitted PCs by the MLR and observation in boreal summer during 1979-1999 (a), and 1999-2010 (b), the common period for the S2S models. Blue curve: MJO-EQBO. Orange curve: MJO-WQBO.